

Enhancement of Power Generation by Capacitive Mixing

by

Thian Xian Khai

15973

Dissertation submitted in partial fulfilment of
the requirements for the
Bachelor of Engineering (Hons)
(Electrical and Electronics)

JANUARY 2016

Universiti Teknologi PETRONAS
Bandar Seri Iskandar
31750 Tronoh
Perak Darul Ridzuan

CERTIFICATION OF APPROVAL
Enhancement of Power Generation by Capacitive Mixing

by

Thian Xian Khai

15973

A project dissertation submitted to the
Electrical and Electronics Engineering Programme
Universiti Teknologi PETRONAS
in partial fulfilment of the requirement for the
BACHELOR OF ENGINEERING (Hons)
(ELECTRICAL AND ELECTRONICS)

Approved by,

(Khairul Nisak Md Hasan)

UNIVERSITI TEKNOLOGI PETRONAS
TRONOH, PERAK
JANUARY 2016

CERTIFICATION OF ORIGINALITY

This is to certify that I am responsible for the work submitted in this project, that the original work is my own except as specified in the references and acknowledgements, and that the original work contained herein have not been undertaken or done by unspecified sources or persons.

THIAN XIAN KHAI

ABSTRACT

This paper is about harnessing blue energy, or salinity gradient power through capacitive mixing and enhancing it by using converters in order to fully utilize the energy obtained from the sea. An experimental setup was done by immersing electrodes of different materials, specifically aluminium and carbon as electrodes into salt water and measuring the obtained voltage and current from the experimental setup. Then, boost and buck converters were designed and simulated in LTSpice in order to determine the most suitable DC-DC converters to be used for this project. The highest obtainable output power from the experiment was 89.7mW. For the simulations, the simulated boost converter was able to boost supply voltage of 1V to 1.61V (theoretical value is 2V) with output current of 160.5mA (load = 10 ohm) and the simulated buck converter was able to step-down supply voltage of 1V to 0.347V (theoretical value is 0.5V) with output current of 34.71mA (load = 10 ohm). By implementing the circuit on PCB, the output voltage obtained was 1.54V with efficiency of 61.54% when compared to the simulated output voltage. The output power per square centimeter was also calculated to be 0.664mW / cm. The experimental setup can be optimized by using different configurations of placement for the electrodes in order to increase the surface area of the carbon to increase the current obtained. Besides that, several cells can be produced and connected in series to obtain higher voltage or connected in parallel for higher current for many other different purposes.

ACKNOWLEDGEMENTS

First and foremost, I would like to give my heartiest appreciation to my supervisor, Madam Khairul Nisak Md Hasan for guiding me along my pathway through Final Year Project 1 and Final Year Project 2. With her advice and guidance, I was able to complete my Final Year Project (FYP). I would also like to express my thanks to the coordinators of FYP 1 and FYP 2 for making it a successful course during my time as a Final Year student.

I would also like to thank my parents for giving me opportunity to pursue Bachelor of Engineering (Honours) Electrical and Electronics in UTP. Without them, I would not be in UTP or completing this FYP. I would also like to thank my family members and friends for giving me moral support during my hardest moments. I was able to be strong and persevere with their supports.

Table of Contents

ABSTRACT.....	i
ACKNOWLEDGEMENTS.....	ii
LIST OF FIGURES.....	v
LIST OF TABLES	vii
ABBREVIATIONS AND NOMENCLATURES	viii
CHAPTER 1 INTRODUCTION	1
1.1 Background.....	1
1.2 Problem Statement	2
1.3 Objectives and Scope of Study	3
CHAPTER 2 LITERATURE REVIEW.....	4
2.1 Pressure-retarded osmosis	4
2.2 Reverse electrodialysis	5
2.3 Capacitive Double Layer Expansion.....	6
2.4 Capacitive Donnan Potential	8
2.5 Mixing entropy battery.....	9
2.6 Comparison between salinity gradient power techniques	10
2.7 Low Voltage Energy Harvesting Circuit.....	12
CHAPTER 3 METHODOLOGY / PROJECT WORK.....	14
3.1 Project Planning	14
3.2 Experimental Setup	15
3.3 DC-DC Converter design and implementation.....	18
3.4 Gantt Chart and Key Milestones.....	21
CHAPTER 4 RESULTS AND DISCUSSION.....	23
4.1 Experimental Results.....	23
4.2 Circuit Simulation Results.....	27
4.3 Circuit Implementation Results	33

4.4 Discussion.....	35
CHAPTER 5 CONCLUSION AND RECOMMENDATIONS	40
References.....	41

LIST OF FIGURES

Figure 1: Citation overview from 1975 to 2011 for the Blue Energy technologies	2
Figure 2: Osmotic Process Plant	5
Figure 3: Reverse electrodialysis (RED) configuration	6
Figure 4: Cell design of CDLE, with black layer as electrodes, grey layer as carbon and blue layer as solution	7
Figure 5: Graph of cell voltage, V_{cell} vs charge, Q	8
Figure 6: Schematic diagram of CDP	9
Figure 7: Working principle for MEB	9
Figure 8: Basic topology of a DC- DC boost converter circuit	12
Figure 9: Mixing entropy battery experimental setup	15
Figure 10: Activated carbon in cloth wrapped in aluminium sheet connected to wire	16
Figure 11: Side view of the interiors of the wrapped up aluminium sheet (left) and front view of the aluminium foil wrappings	16
Figure 12: No continuity between anode and cathode	17
Figure 13: Tank filled with salt water	17
Figure 14: Measuring beaker	17
Figure 15: Experimental setup of the cell	18
Figure 16: Boost converter circuit implemented on breadboard for testing	20
Figure 17: Multimeter probes connected to the cell	23
Figure 18: Measured voltage	23
Figure 19: Measured current	24
Figure 20: Schematic diagram for simulated boost converter using LTSpice	27
Figure 21: Graph of V_{out} and V_{in} for simulated boost converter circuit	28
Figure 22: Voltage values for both V_{in} ($V(n001)$) and V_{out} ($V(out)$) for boost converter	29
Figure 23: Graph of I_{out} [$I(R1)$] and I_{in} [$I(L1)$] for simulated boost converter circuit	29
Figure 24: Schematic diagram for simulated buck converter using LTSpice	30
Figure 25: Voltage values for both V_{in} ($V(n001)$) and V_{out} ($V(out)$) for buck converter	30
Figure 26: Graph of V_{in} and V_{out} for simulated buck converter circuit	31

Figure 27: Graph of I_{out} [$I(R1)$] and I_{in} [$I_d(M1)$] for simulated buck converter circuit	32
Figure 28: Implemented boost converter	33
Figure 29: Input voltage of 1.025V measured	33
Figure 30: Output voltage of 1.258V measured	33
Figure 31: Graph of output voltage against time for different concentration of solute	35
Figure 32: Graph of output voltage against time for different volumes of water	36
Figure 33: Graph of output voltage against time for different types of electrolyte	36
Figure 34: Graph of output power against time for different concentration of solute	37
Figure 35: Graph of output power against time for different volume of water	37
Figure 36: Graph of output power against time for different types of electrolyte	38

LIST OF TABLES

Table 1: Characteristics Comparison of Salinity Gradient Power Techniques	10
Table 2: Parameters for boost and buck converters	19
Table 3: Experimental results for NaCl electrolyte with different levels of mass and concentration for NaCl but same volume of water	24
Table 4: Experimental results for NaCl electrolyte with same concentration of NaCl (1.677 M) but different volume of water	25
Table 5: Experimental results for different types of electrolytes	26
Table 6: Voltage, current, power and efficiency for designed boost converter	34

ABBREVIATIONS AND NOMENCLATURES

RED – Reversed Electrodialysis

PRO – Pressure Retarded Osmosis

CDLE – Capacitive Double Layer Expansion

CDP – Capacitive Donnan Potential

MEB – Mixing Entropy Battery

CAPMIX – Capacitive Mixing

AEM – Anion Exchange Membrane

CEM – Cation Exchange Membrane

EDL – Electric Double Layers

CCM – Continuous Conduction Mode

DCM – Discontinuous Conduction Mode

PCB – Printed Circuit Board

CHAPTER 1

INTRODUCTION

1.1 Background

The world's increasing demand for energy encourages the use of renewable energy as an alternative to fossil fuels that are getting scarce. Renewable energy is also important to reduce pollution and carbon emission caused by the usage of fossil fuels as energy sources. Renewable energies such as solar, wind, geothermal and tidal energy are widely researched and used both in commercial and private sectors. However, another source of renewable energy called "Blue Energy" [1] or better known as salinity gradient power is a potential renewable energy that has yet to be fully utilized. Salinity gradient power relies on the different salt concentration in saltwater and freshwater to generate energy. When the mixing of seawater and freshwater occurs, an increase in the entropy of this system is observed and free energy is dissipated. This renewable energy is clean and green [2] as it does not produce any wastes that may cause environmental pollution. Globally, with an estimated 2.6 TW [3] of energy output from blue energy, this renewable energy will be able to provide a significant amount of the global energy needs.

In order to harness blue energy, many techniques were developed. All of these techniques have different working principles or power generation mechanism. Five different techniques in extracting blue energy will be discussed, which are: Reversed Electrodialysis (RED) [1, 4, 5], Pressure Retarded Osmosis (PRO) [1, 2, 5], Capacitive Double Layer Expansion (CDLE) [5, 6], Capacitive Donnan Potential (CDP) [6, 7] and Mixing Entropy Battery (MEB) [5]. Three of the techniques, which are CDLE, CDP and MEB are under capacitive mixing (CAPMIX) category. All these techniques will be further elaborated in the literature review.

1.2 Problem Statement

Due to the energy crisis in 1973, research on salinity gradient power increases during the 1970's. As mentioned by Jones and Finley [2], the research and development of blue energy for the past thirty years had been lacking. This is mainly due to several reasons such as cost effectiveness and underexplored technology. In this research, the problem statement is the non-economical energy production based on current methods of harvesting blue energy. The current methods such as PRO and RED requires expensive membranes. According to Gerstandt et al., for PRO to be profitable, a breakeven point of 5 W/m² for the power density of the membrane was decided. However, the highest power density per membrane obtained from experimental was 3.5 W/m². [8] Similar situation was also observed for RED. So, this research focuses on techniques under CAPMIX and ways to increase the power generation.

Besides having cost effectiveness as a commercial barrier, blue energy is still a developing technology. Based on the statistics [6] given by Bijmans et al., CAPMIX methods are still novel, which can be seen by the number of publications, especially the MEB method. The lack of publications done on MEB method suggests that the method itself is still underdeveloped and requires extensive research.

In enhancement of the energy harvested, a suitable circuit is also required in order to ensure that the blue energy can be utilized efficiently by boosting it and storing the energy into storage such as capacitors.

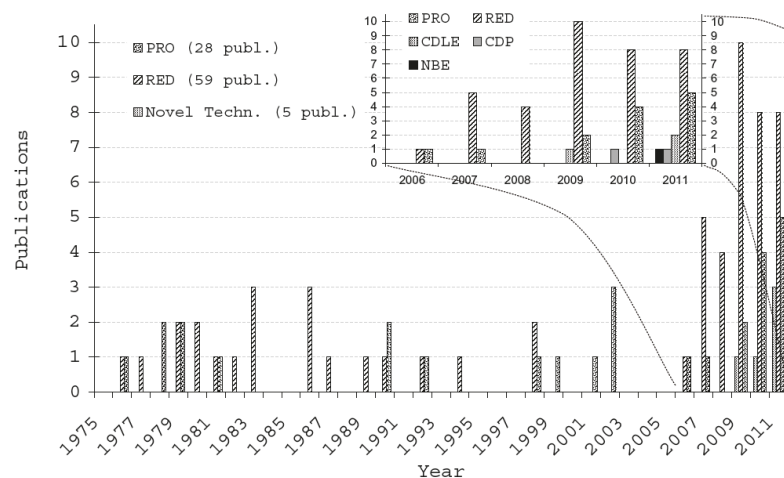


Figure 1: Citation overview from 1975 to 2011 for the Blue Energy technologies [6]

1.3 Objectives and Scope of Study

The objectives of this research are as follows:

1. To investigate and identify the method to increase the power generated by capacitive mixing.
 - Research and study will be done on listed techniques based on salinity gradient power
 - Comparison between these techniques will be done and the best method will be chosen
 - Alternatives to increase the output power will be done based on electronic circuits
2. To conduct an experiment to verify the identified method.
 - Experiment will be conducted to obtain experimental results and comparison with theoretical values will be done
 - Based on experimental results, the identified method will be verified accordingly and conclusion will be done

CHAPTER 2

LITERATURE REVIEW

In general, there are five different techniques in harvesting salinity gradient power. Three of these techniques uses membranes; pressure-retarded osmosis, reverse electrodialysis and capacitive Donnan potential. The other two methods, capacitive double layer expansion and mixing entropy battery does not require membranes for the energy extraction, but instead relies on capacitors and Donnan Potential. Each techniques have their own working principles, pros and cons in extraction of salinity gradient power.

2.1 Pressure-retarded osmosis

First discovered by Sidney Loeb in 1973, pressure-retarded osmosis (PRO) is a method that extracts the osmosis pressure difference between seawater and freshwater. By utilizing a semi-permeable membrane, this pressure difference can be used in power generation. Based on Figure 2, the PRO process can be summarized as below:

1. From the inlets, both seawater and freshwater enters the system and undergo filter process before reaching the chamber with membrane modules.
2. The sea water which has higher concentration of salt will be pressurized by the pressure exchanger before reaching the membrane module.
3. When both the pressurized seawater and freshwater meets together at the membrane module, osmosis occurs in which the freshwater will diffuse to the pressurized seawater, increasing the static energy at the higher concentration side.
4. This mixture of seawater and freshwater called brackish water will be divided into two streams, one stream going to the pressure exchanger to pressurize incoming sea water while the other stream will be depressurized by hydropower turbine to generate electricity.

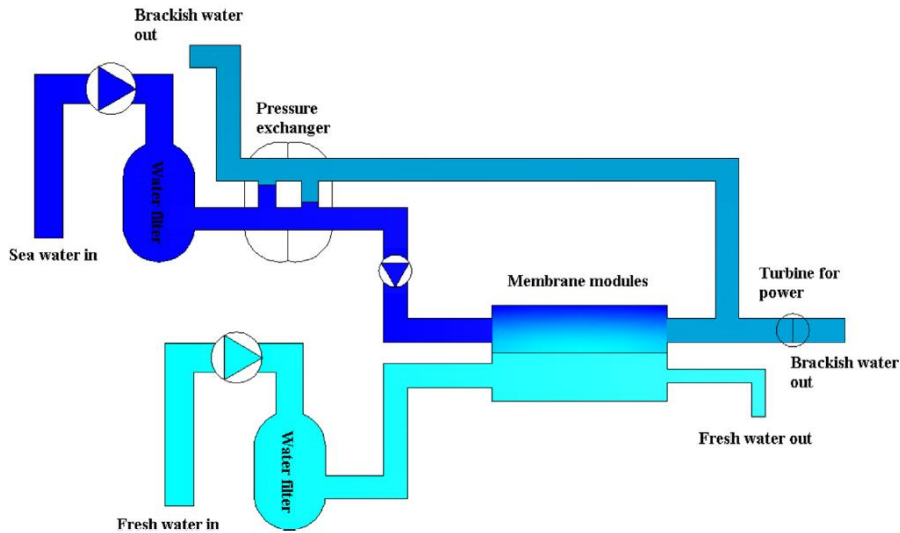


Figure 2: Osmotic Process Plant [5]

By observing the process shown in the Figure 2, we can conclude that the power obtained from PRO depends on the efficiency of the membrane and the pressure exchanger. According to Thorsen and Holt, 1 MW can be generated from each cubic metre per second of freshwater that mixes with seawater if membranes optimized for PRO is created based on the semi-permeable properties of the best commercial RO membrane [9].

A pilot plant for power generation thorough PRO was commissioned at Tofte, Norway on 24th November 2009. The pilot plant was said to have the capacity of 4 kW only. The membrane used by the pilot plant can only generate roughly 1 W/m² [5], which is far lower than the targeted power density of 5 W/m². This means that that membrane was unable to reach an economical break-even for the power generated per square metre and cost of the membrane. As a result, an economical barrier prevents the PRO from being a cost-effective method of generating power. Similar research is also being done for the PRO system by a prototype plant in Fukuoka, Japan to utilize the energy recovery of the process and treatment of brine water to prevent environmental issues [10].

2.2 Reverse electrodialysis

This method is introduced by Pattle as reverse electrodialysis (RED) [11]. In RED, two different types of membranes: anion exchange membrane (AEM) and cation exchange membrane (CEM) are stacked alternately between each other and placed

in between an anode and a cathode. By flushing salt water and fresh water thorough the space in between these membranes as shown in Figure 3, electrochemical potential is produced due to concentration difference between the solutions and ion-selectivity of the membranes [5]. Positive ions, Na^+ will diffuse thorough the CEM while the Cl^- will diffuse thorough the AEM. The movement of these ions will produce ionic current and thus generating power.

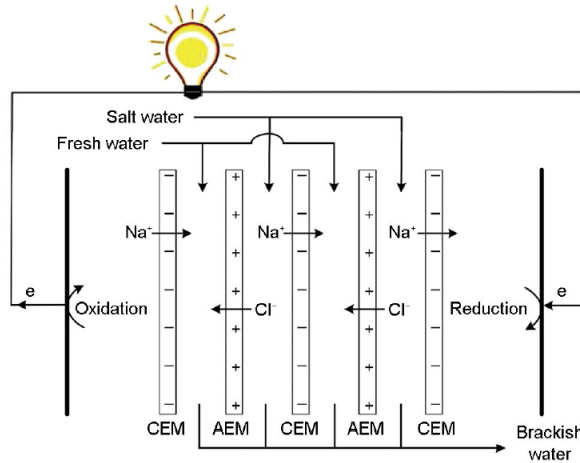


Figure 3: Reverse electrodialysis (RED) configuration [4, 12]

In a research done by Z. Jia et al. [5], experimental results showed a power density of 0.93 W/m^2 based on artificial seawater and river water. This result is not up to the targeted power density needed in order for RED to be economical in commercial uses.

Currently, there is a pilot plant located at Afsluitdijk, the Netherlands which harvests salinity gradient power through RED. This plant is operated by a company called RedStack. The plant is expected to produce 50 kW blue-energy per hour, aiming to raise the output to 200 kW per plant. As mentioned by Schaetzle and Buisman [12], the RedStack engineers must overcome challenges in implementing RED technology in the real environment as opposed to controlled environment in the laboratory where conditions in the real environment might not be favorable for RED technology.

2.3 Capacitive Double Layer Expansion

Two electrodes are immersed into an ionic solution such as salt water to form a super capacitor. When the electrodes are connected to power supply and charged,

electrical charge is stored in the electric double layers (EDL) between the carbon and solution. When the salinity of the solution decreases, the potential difference across EDLs increases with constant charge. This occurs due to counter-ions in the EDL moving away from the electrode using free energy of the solutions, hence this technique is named “capacitive double layer expansion” (CDLE).

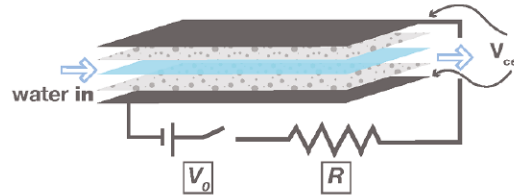


Figure 4: Cell design of CDLE, with black layer as electrodes, grey layer as carbon and blue layer as solution [6]

The following are steps to replicate the CDLE phenomenon:

- A. The electrodes which are immersed in salt water are connected to external power supply to charge.
- B. After charging, the circuit is disconnected from the power supply and become open circuit.
- C. The salt water is replace with freshwater and a load is added to discharge the cell.
- D. After that, the circuit is opened again and the freshwater is replace with salt water again.

Based on the steps given, graph of cell voltage, V_{cell} vs charge, Q was plotted. Stored charges were retrieved in Step C at a higher potential difference as compared to Step A. As a result, an area was formed under the plotted curve; which was the energy extracted by CDLE.

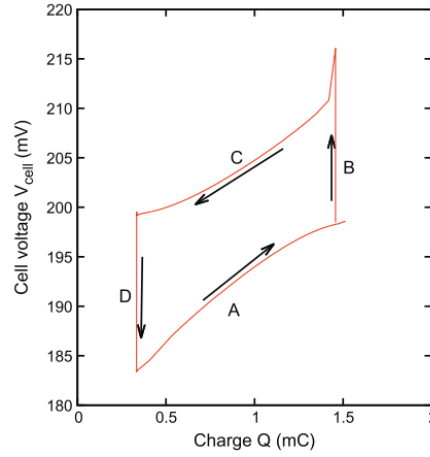


Figure 5: Graph of cell voltage, V_{cell} vs charge, Q [13]

An experiment was done by D. Brogioli, et al. [14], in which the highest power density of 50 mW/m^2 was produced using A-PC-2 and NS30 as activated carbon materials. Brogioli, et al. said that in order to improve the energy extraction thorough CDLE, we should use different materials for positive electrodes and negative electrodes. When two electrodes with different potential rises were used, the cell will experience a voltage rise, or called “zero charging” in which no external supply was needed for charging and discharging phase.

2.4 Capacitive Donnan Potential

Another technique which are based off CDLE is called Capacitive Donnan Potential (CDP). This technique is similar to CDLE, but with one major difference; the usage of membranes. In CDLE, no membranes are used to extract the salinity gradient energy but for CDP, layers of AEM and CEM in between the layer of carbon and water flow. As a result, when water seawater flows through, ions from the concentrated seawater diffuse thorough the AEM and CEM into the electrodes. This movement of ions will produce current to an external load. After reaching equilibrium, freshwater will flow into the system and the ions inside the electrodes and membranes will diffuse out to form current in the opposite direction.

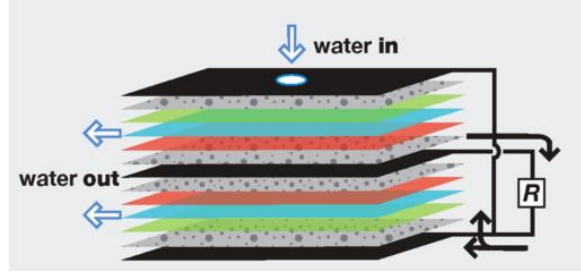


Figure 6: Schematic diagram of CDP [15]

Based on a research done by B.B. Sales et al. [7], maximum power density of 131.7 mW/m^2 was reached and an average power of 8.36 mW/m^2 was produced for one cycle of CDP technique. Optimization of distance between the electrodes in respect to the hydrodynamics of the flow of solution is recommended by them in order to improve this technique.

2.5 Mixing entropy battery

In mixing entropy battery (MEB) or sometimes known as faradaic pseudo capacitor [5], the energy is extracted from salinity difference between two solutions and stored inside the electrode. By using battery-like electrodes, the ions are captured in the solution through redox reactions [16]. The voltage of the electrodes used changes with respect to the solution and this will reflect ions' the chemical potential in the solution.

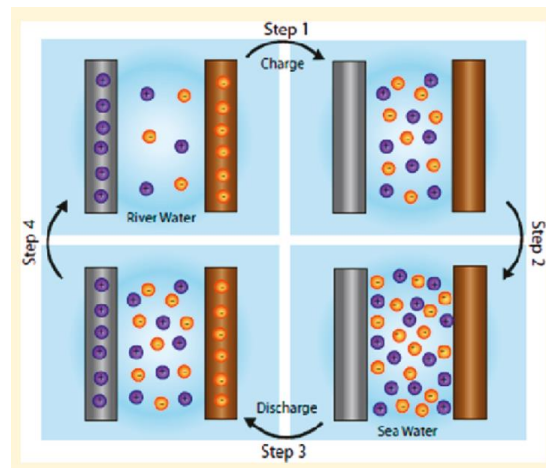


Figure 7: Working principle for MEB [17]

In step 1, the electrodes are immersed into a low concentration solution such as river water, in which the battery is charged and the ions are removed from the

electrodes. In step 2, the river water is exchanged with sea water which has higher concentration of ions and thus higher potential difference between the electrodes. The battery is discharged as shown in step 3 and the ions are restored into the electrodes. Finally in step 4, the seawater is flushed out and replaced with river water which results in decrement of potential difference between the electrodes. In step 2 and 4, energy is not absorbed or released. However, in step 1 energy is consumed to release the ions from the structure while in step 3, energy is produced due to the incorporation of the ions into the electrodes. Due to the fact that same amount of charge moves in and out of the electrodes during step 1 and 3 but at higher potential difference in step 3 with respect to step 1, there will be energy gained.

In an experiment done by F. L. Mantia et al., they managed to produce power density of 138 mW/cm². The process was repeated for over 100 cycles (times) and the power density produced was stable. As mentioned, MEB might be a potential technique to harness blue energy due to the renewable nature of this technique; no loss of reagent even with repeated usage of the materials in MEB.

2.6 Comparison between salinity gradient power techniques

The following are tables of comparison between different techniques for salinity gradient power. Comparisons are made based on techniques, type, membrane characteristics, researches and reviews.

Table 1: Characteristics Comparison of Salinity Gradient Power Techniques

Technique	Type	Membrane Characteristics	Researches		Reviews
			Author	Reference No.	
Pressure-retarded osmosis	Osmotic pressure difference (Mechanical)	Water selective	Thor Thorsen, Torleif Holt	[9]	- Power density of roughly 1 W/m ² produced - Pilot plant available in Norway - Translates to pressure difference
			K. Gerstandt, K. V. Peinemann, S. E. Skilhagen, T. Thorsen, and T. Holt	[8]	
			J. W. Post, J. Veerman, H. V. M. Hamelers, G. J. W. Euverink, S. J. Metz, K. Nymeijer, et al.	[1]	

					equivalent in hydraulic head
Reverse Electrodiagnosis	Electrochemical reactions	Ionic selective	Z. Jia, B. Wang, S. Song, and Y. Fan	[5]	- Produced power density of 0.93 W/m ² - Pilot plant available in the Netherlands
			J. W. Post, J. Veerman, H. V. M. Hamelers, G. J. W. Euverink, S. J. Metz, K. Nijmeijer, et al.	[1]	
			D. A. Vermaas, E. Guler, M. Saakes, and K. Nijmeijer	[4]	
Capacitive Double Layer Expansion	Ultra Capacitor	None	D. Brogioli, R. Ziano, R. A. Rica, D. Salerno, O. Kozynchenko, H. V. M. Hamelers, et al.	[14]	- Power density of 50 mW/m ² produced in lab setups - Not commercialize and currently only in experimental scale - Does not require membrane
			M.F.M. Bijmansa, O.S. Burheim, M. Bryjak, A. Delgado, P. Hack, F. Mantegazza, S. Tenisson, H.V.M. Hamelers	[6]	
			D. Brogioli, R. Ziano, R. A. Rica, D. Salerno, and F. Mantegazza	[13]	
Capacitive Donnan Potential	Ultra Capacitor	Ionic selective	B. B. Sales, M. Saakes, J. W. Post, C. J. N. Buisman, P. M. Biesheuvel, and H. V. M. Hamelers	[15]	- Maximum power density of 131.7mW/m ² produced per cycle in lab setup - Similar concept to CDLE with membrane usage
			B. B. Sales, F. Liu, O. Schaetzle, C. J. N. Buisman, and H. V. M. Hamelers	[7]	
			M.F.M. Bijmansa, O.S. Burheim, M. Bryjak, A. Delgado, P. Hack, F. Mantegazza, S. Tenisson, H.V.M. Hamelers	[6]	

Mixing Entropy Battery (Nano Battery Electrodes)	Electrochemical reactions	None	F. La Mantia, M. Pasta, H. D. Deshazer, B. E. Logan, and Y. Cui	[16]	- Power density of 138mW/m ² was reached in small lab scale -Uses different types of electrodes for anode/cathode
			Z. Jia, B. Wang, S. Song, and Y. Fan	[5]	

2.7 Low Voltage Energy Harvesting Circuit

The techniques mentioned above produces low voltage and current. With low supply of energy, they are unsuitable to be used for electronic devices and many other applications. So, in order to utilize the blue energy, an electronic circuit is required. According to N. A. C. Mustapha, et al. [18], power switching converter circuit such as buck and boost converters are needed. A DC-DC converter is normally used in order to step-up or step-down the voltage from energy harvest methods.

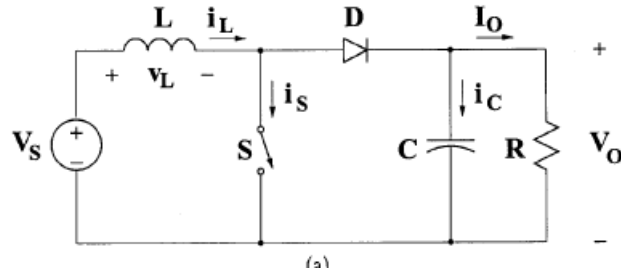


Figure 8: Basic topology of a DC- DC boost converter circuit [19]

In a boost converter, the relationship between input voltage V_s , output voltage V_o and duty cycle of switch D can be derived, and using Faraday's Law, the following equation is obtained:

$$V_s D T = (V_o - V_s)(1 - D)T$$

from which the ratio between output voltage and input voltage can be obtained:

$$\frac{V_o}{V_s} = \frac{1}{1 - D}$$

For the buck converter, according to Faraday's Law, the following equation can be obtained:

$$(V_s - V_o)DT = -V_o(1 - D)T$$

in which the ratio between output voltage and input voltage can be obtained:

$$\frac{V_o}{V_s} = D$$

Based on these equations, it can be concluded that the output voltage can be manipulated by changing the switch duty ratio D .

A DC-DC converter can operate both in Continuous Conduction Mode (CCM) and Discontinuous Conduction Mode (DCM) with respect to the inductor current, i_L . In CCM, the inductor current is always greater than zero while in DCM, the inductor current is zero during a portion of the switching period, which may occur due to low value of the average output current or low switching frequency. CCM is desired due to the high efficiency and decent operation of switches and components. For the converters to always operate in CCM mode, there must be a minimum inductance value L required called the boundary inductance value L_b . The converters required the value of $L > L_b$ to ensure the converter operates in CCM mode. Other design parameters such as the capacitance value will affect the output ripple voltage. Normally, a boost converter circuit will require larger filter capacitor compared to buck converters to limit the output ripple voltage. A suitable resistance value must also be chose as the load so that the output current is not too low, which will cause the converter to enter DCM. [19].

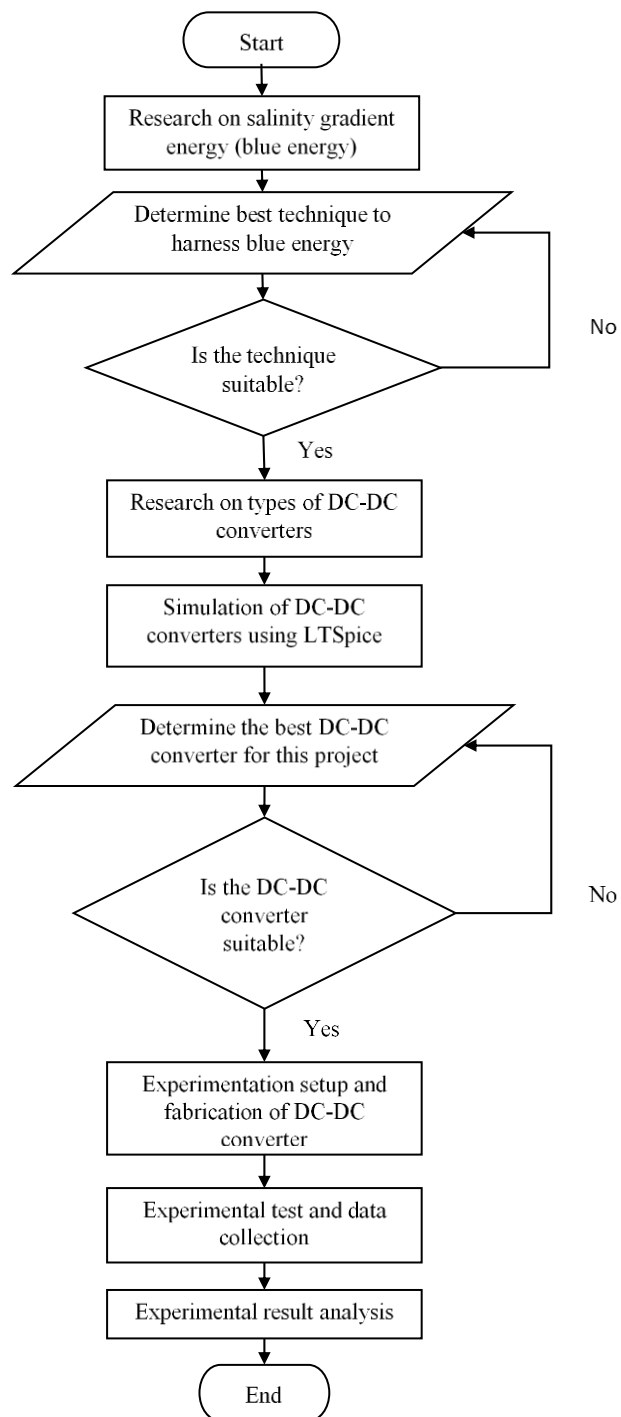
According to M.R. Sarker, et al. [20], most of the energy harvesting circuit involves power levels that are low, in which a low power consumption circuit must be designed and used to avoid the loss of already low level power harvested by these methods. DC-DC step down converters were mentioned to be a low performance circuit that can be used in energy harvesting circuit. Besides that, D. Dondi, et al. [21] uses different topology for their low energy harvesting circuit. In their paper, a step-up voltage regulator was used instead of a step-down converter. The step-up voltage regulator was also efficient due to the implementation of a system in which it will not be turned on if the starting voltage is below the specified voltage. This is done to avoid consummation of power even if the circuit is not boosting the output voltage.

CHAPTER 3

METHODOLOGY / PROJECT WORK

3.1 Project Planning

The following is a flowchart for the project which outlines the work done for the project:



3.2 Experimental Setup

The following Figure 8 is a representative of how a mixing entropy experimental cell look like:

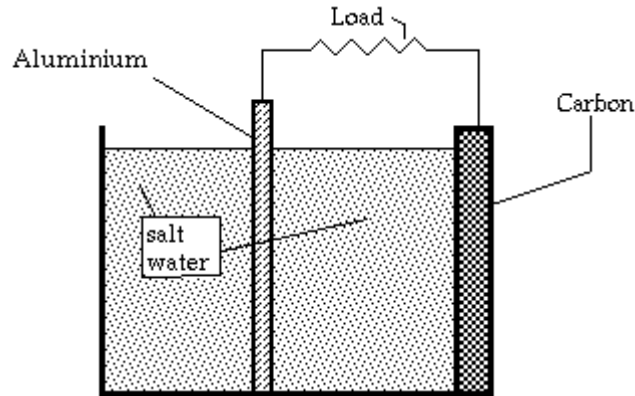
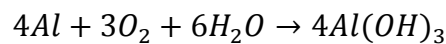


Figure 9: Mixing entropy battery experimental setup

Two electrodes, an aluminium electrode and a carbon electrode is prepared. A solution of salt water is also prepared by dissolving salt into water. When the aluminium electrode and carbon electrode are immersed into the salt water, a redox reaction occurs according to the following chemical reaction:



The open circuit voltage V_{oc} or the potential difference between the two electrodes can be measured by taking out the load and connecting it to the multimeter. The current can be measure by applying load or resistance in between the two terminals (both aluminium and carbon electrodes). In order to increase the voltage or current, multiple cells can be connected in series to increase the voltage or connected in parallel to increase the current.

The following are the steps in conducting the experiment:

1. Prepare an aluminium electrode and a carbon electrode.
2. Add 5.2 teaspoons of table salt (roughly 1 mole) to water. Stir until the table salt dissolved completely.
3. Immerse the electrodes into the salt water.
4. Connect the probe end of multimeter or load to take voltage and current readings.

An experimental setup similar to Figure 9 was set up. Activated carbon powder were filled into layers of cloth (as a hydrophobic membrane between carbon and aluminium) connected with a multi-cores wire and an aluminium foil was wrapped around the cloth as shown in Figure 10 and Figure 11. The aluminium foil acted as anode while the activated carbon acted as air cathode. Two wires, both anode and cathode was attached to the current collector and aluminium foil.

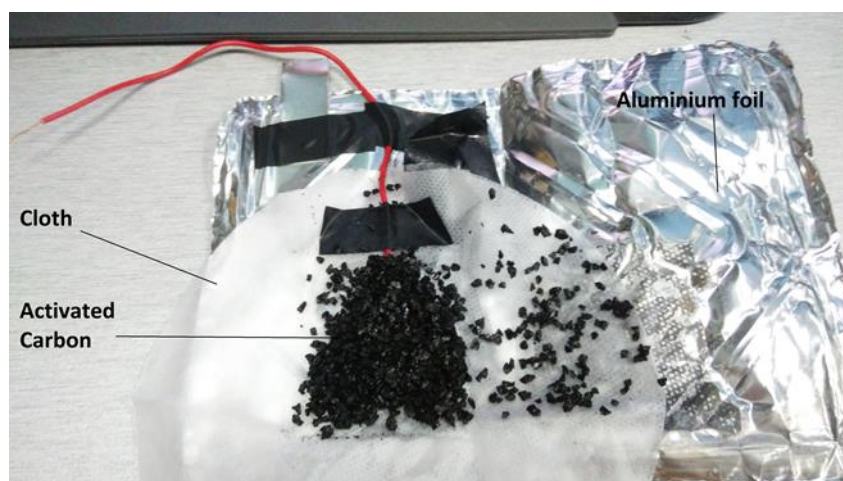


Figure 10: Activated carbon in cloth wrapped in aluminium sheet connected to wire

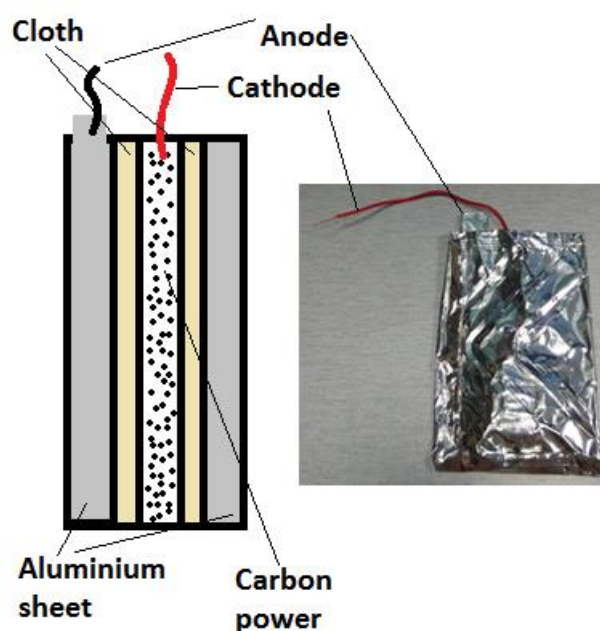


Figure 11: Side view of the interiors of the wrapped up aluminium sheet (left) and front view of the aluminium foil wrappings

No continuity was allowed between the anode and cathode before experiment by testing using the multimeter as shown in Figure 12. This is to prevent the anode and cathode from short-circuiting.



Figure 12: No continuity between anode and cathode

A tank filled with salt water was prepared as shown in Figure 13 by using the right amount of salt and water which were measured through a measuring beaker as shown in Figure 14.



Figure 13: Tank filled with salt water



Figure 14: Measuring beaker

The full experiment setup is as shown in Figure 15, and both ends of the anode and cathode were connected to multimeter for measuring and collecting data.

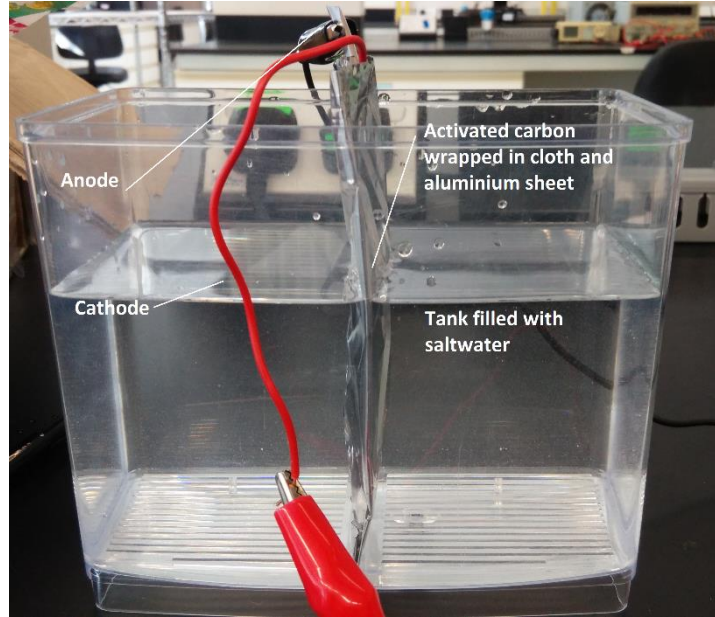


Figure 15: Experimental setup of the cell

3.3 DC-DC Converter design and implementation

For the DC-DC converter design, a simple design will be used based on the most basic topology of converter as shown in Figure 8 in the Literature Review section. The parameters that will be decided in the design includes the inductance value (H) to be used, switching frequency for the transistors (Hz), load resistance value (ohm), duty cycle of the transistors and capacitance value (F) to be used. In order to maintain the continuous conduction mode for the converters, the value of inductance used must exceed the boundary inductor value, $L > L_b$ as shown in the following equation:

For boost converter,

$$L_b = \frac{(1 - D)^2 DR}{2f}$$

For buck converter,

$$L_b = \frac{(1 - D)R}{2f}$$

The switching frequency used for both types of converters are the same, which is $f = 100 \text{ kHz}$. The load resistance for the boost converter circuit is $R_{\text{boost}} = 1 \text{ k ohm}$ while for the buck converter, $R_{\text{buck}} = 10 \text{ ohm}$. The duty cycle of the transistors can be adjusted depending on ratio between output voltage desired and input voltage. For the capacitance value, the capacitance value is chosen based on the % of output ripple voltage (V_r/V_o) required and using the following equation:

For boost converter,

$$C_{\min} = \frac{DV_o}{V_r R f}$$

For buck converter,

$$C_{\min} = \frac{(1 - D)V_o}{8V_r L f^2}$$

The parameters used in the simulation for the converters are shown in Table 2.

Table 2: Parameters for boost and buck converters

Parameters	Boost Converter	Buck Converter
Inductance value (H)	625 μ H	47 μ H
Switching frequency for the transistors (Hz)	100kHz	100kHz
Load resistance value (ohm)	1k ohm	10 ohm
Duty cycle of the transistors	0.5	0.5
Capacitance value (F)	0.5 μ F	100 μ F

Before prototyping of the converter for the circuit, different topologies of converters are simulated using LTSpice. Basic topology of both step-up (boost) converter and step-down (buck) converter [19] will be compared to find out the optimum converter to be used in harnessing energy through capacitive mixing. To design the converter, LTSpice will be used to simulate the circuit by using different

parameters in order to decide which parameters are suitable. Data and results from the simulation will be recorded. After designing the circuit in LTSpice, the physical implementation of the circuit will be done on printed circuit board (PCB). All the components will be tested and implemented on the PCB by soldering them according to schematics from the LTSpice. After implementation of the components on the PCB, testing of the circuit will be done to obtain data and experimental results. These results will be compared with theoretical or simulation results in order to validate them. Improvement or optimization will be done after validation of a working DC-DC converter.

As mentioned, the physical implementation of the boost converter simulated through LTSpice were done by using the following list of components:

1. Voltage supply
2. Function generator
3. 10 μ H Inductor
4. 1N5819 Diode
5. IRFZ24N Transistor N Channel Power MOSFET
6. 100 μ F Capacitor
7. 10 ohm Resistor

The circuit were implemented on breadboard for testing purposes before the implementation of it on PCB as shown in Figure 16.

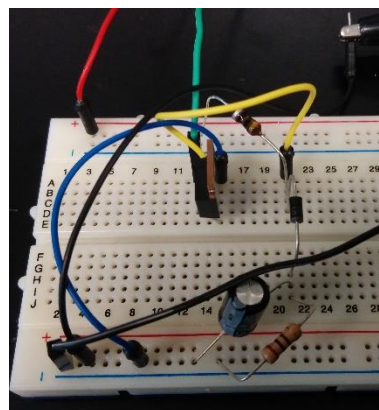


Figure 16: Boost converter circuit implemented on breadboard for testing

3.4 Gantt Chart and Key Milestones

FYP 1 Timeline

No.	Detail /Week	1	2	3	4	5	6	7	8	9	10	11	12	13	14
1.	Defining project title	■	■												
2.	Literature review on salinity gradient power			■	■	■									
3.	Research on PRO,RED,CDLE,CDP and MEB techniques			■	■	■									
4.	Research on circuit designs for low voltage application (SGP)				■	■									
5.	Extended proposal preparation			■	■	■									
6.	Submission of extended proposal						■								
7.	Designing DC-DC converters using LTSpice						■	■							
8.	Proposal defense								■	■					
9.	Finalizing circuit design with parameters and experimental setup preparation									■	■	■	■		
10.	MEB experimental setup and testing												■	■	
11.	Interim draft submission														■
12.	Final interim report submission														■

Key Milestones



1. Submission of Extended Proposal – Week 6

2. Submission of Interim Draft Report – Week 13

3. Submission of Interim Report – Week 14

FYP Timeline 2

No.	Detail /Week	1	2	3	4	5	6	7	8	9	10	11	12	13	14	15
1.	Simulation of converter design using LTSpice															
2.	Implementation of boost converter circuit based on design															
3.	Circuitry testing and data collection on voltage and current output															
4.	Progress report submission															
5.	Comparison between theoretical and experimental results															
6.	Optimization of circuit based on obtained results															
7.	Pre-SEDEX															
8.	Final report draft submission															
9.	Soft bound dissertation submission															
10.	Technical paper submission															
11.	Viva															
12.	Hard bounded project dissertation submission															

Key Milestone



1. Progress Report Submission – Week 7
2. Pre-SEDEX – Week 10
3. Draft Final Report Submission – Week 11
4. Soft-bounded Dissertation Submission – Week 12
5. Technical Paper Submission – Week 12
6. Viva – Week 13
7. Project Dissertation (Hard Bound) Submission – Week 15

CHAPTER 4

RESULTS AND DISCUSSION

4.1 Experimental Results

A multimeter was used to measure the voltage and current of the cell. Figure 17 shows the measurement being taken by connecting the probe to the anode and cathode wires while Figure 18 shows the measured voltage obtained from the multimeter.

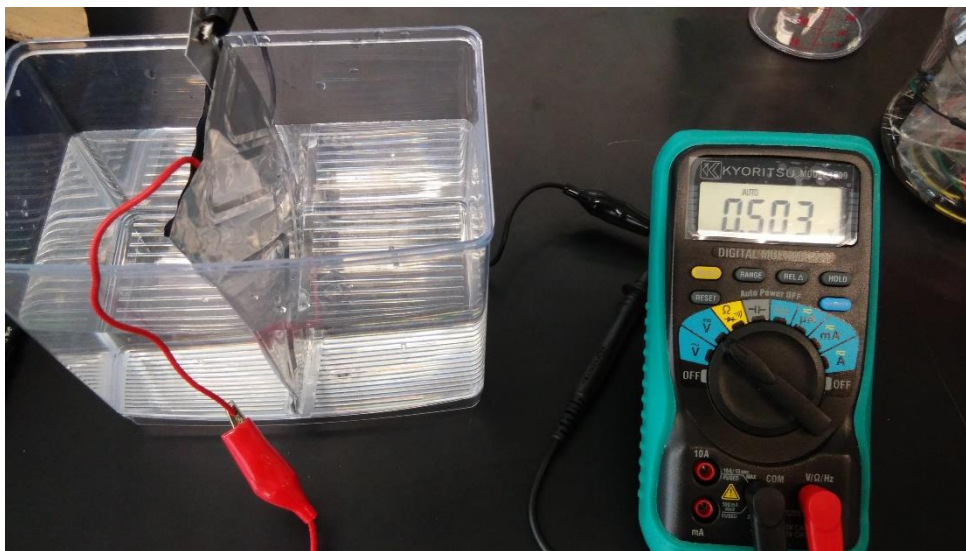


Figure 17: Multimeter probes connected to the cell



Figure 18: Measured voltage

Besides measuring voltage, the current of the cell was also measured using the multimeter as shown in Figure 19.

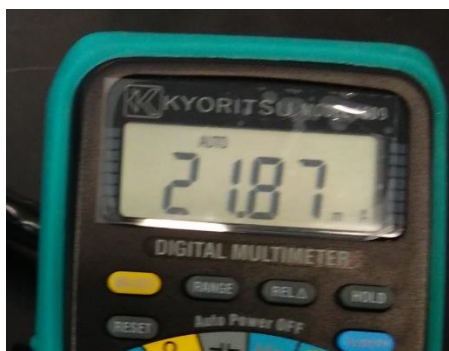


Figure 19: Measured current

Different parameters such as concentration of solute, volume of water and type of electrolytes were used as variables in the experiment. The readings for both voltage and current were tabulated in Table 3, Table 4 and Table 5 with different variables for each table.

Table 3: Experimental results for NaCl electrolyte with different levels of mass and concentration for NaCl but same volume of water

Type of Electrodes	Volume of Water (ml)	Type of Electrolyte	Mass (g) & Concentration of Solute (M)	Time (min)	Voltage (V)	Current (A)	Power (W)
Carbon – Aluminium	1000 ml	NaCl	35g Concentration = 0.624 M	5	0.503	21.87m	11.0m
				10	0.280	14.15m	3.96m
				15	0.253	13.14m	3.32m
				20	0.214	11.22m	2.40m
				25	0.194	9.21m	1.79m
				30	0.162	4.44m	0.72m
Carbon – Aluminium	1000 ml	NaCl	100g Concentration = 1.677 M	5	0.547	56.20m	30.7m
				10	0.492	46.90m	23.1m
				15	0.479	45.90m	22.0m
				20	0.443	35.90m	15.9m
				25	0.420	27.00m	11.3m
				30	0.384	24.13m	9.27m
Carbon – Aluminium	1000 ml	NaCl	250g Concentration = 3.690 M	5	0.627	66.10m	41.4m
				10	0.413	52.10m	21.5m
				15	0.418	45.30m	18.9m
				20	0.361	42.50m	15.3m
				25	0.336	23.33m	7.84m
				30	0.316	21.09m	6.66m

Table 4: Experimental results for NaCl electrolyte with same concentration of NaCl (1.677 M) but different volume of water

Type of Electrodes	Volume of Water (ml)	Type of Electrolyte	Mass (g) & Concentration of Solute (M)	Time (min)	Voltage (V)	Current (A)	Power (W)
Carbon – Aluminium	500 ml	NaCl	50g Concentration = 1.677 M	5	0.522	48.90m	25.5m
				10	0.511	47.80m	24.4m
				15	0.504	44.90m	22.7m
				20	0.496	41.50m	20.6m
				25	0.494	39.20m	19.4m
				30	0.485	37.60m	18.2m
Carbon – Aluminium	750 ml	NaCl	75g Concentration = 1.677 M	5	0.616	47.00m	29.0m
				10	0.477	45.10m	21.5m
				15	0.501	44.70m	22.4m
				20	0.453	41.80m	18.9m
				25	0.494	43.80m	21.6m
				30	0.449	42.10m	18.9m
Carbon – Aluminium	1000 ml	NaCl	100g Concentration = 1.677 M	5	0.557	56.50m	31.5m
				10	0.501	47.00m	23.5m
				15	0.453	46.00m	20.8m
				20	0.433	37.00m	16.0m
				25	0.410	26.90m	11.0m
				30	0.385	24.15m	9.3m

Table 5: Experimental results for different types of electrolytes

Type of Electrodes	Volume of Water (ml)	Type of Electrolyte	Mass (g) / Volume & Concentration of Solute (M / %)	Time (min)	Voltage (V)	Current (A)	Power (W)
Carbon – Aluminium	500 ml	Water	-	5	0.677	0.00m	0
				10	0.580	0.00m	0
				15	0.546	0.00m	0
				20	0.501	0.00m	0
				25	0.454	0.00m	0
				30	0.437	0.00m	0
Carbon – Aluminium	500 ml	NaCl	50g Concentration = 1.677 M	5	0.521	48.70m	25.4m
				10	0.510	47.70m	24.3m
				15	0.503	45.00m	22.6m
				20	0.497	41.60m	20.7m
				25	0.494	40.20m	19.9m
				30	0.486	37.62m	18.3m
Carbon – Aluminium	500 ml	Water and Vinegar (Acetic Acid)	100 ml Concentration = 20%	5	0.794	113.0m	89.7m
				10	0.551	77.30m	42.6m
				15	0.570	68.20m	38.9m
				20	0.499	56.50m	28.2m
				25	0.521	50.40m	26.3m
				30	0.468	46.50m	21.8m

The voltage and current readings taken and tabulated were analyzed in the discussion section.

4.2 Circuit Simulation Results

In order to decide on the type of DC-DC converters to be used, the converters must be simulated using LTSpice based on the output from the experiment done. Figure 20 shows the schematic diagram for the boost converter simulated using LTSpice. A MOSFET is used as the switching component, with a pulse generator as the gate driver.

Boost Converter

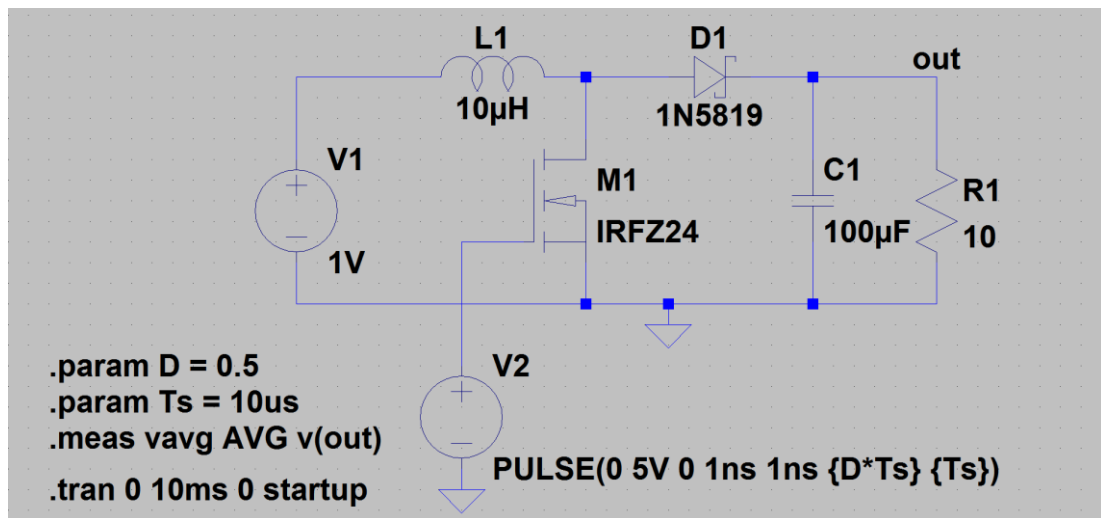


Figure 20: Schematic diagram for simulated boost converter using LTSpice

The simulation was done and a graph of V_{out} and V_{in} was obtained from the simulation as shown in Figure 21. The voltage readings obtained can be seen clearly in Figure 22.

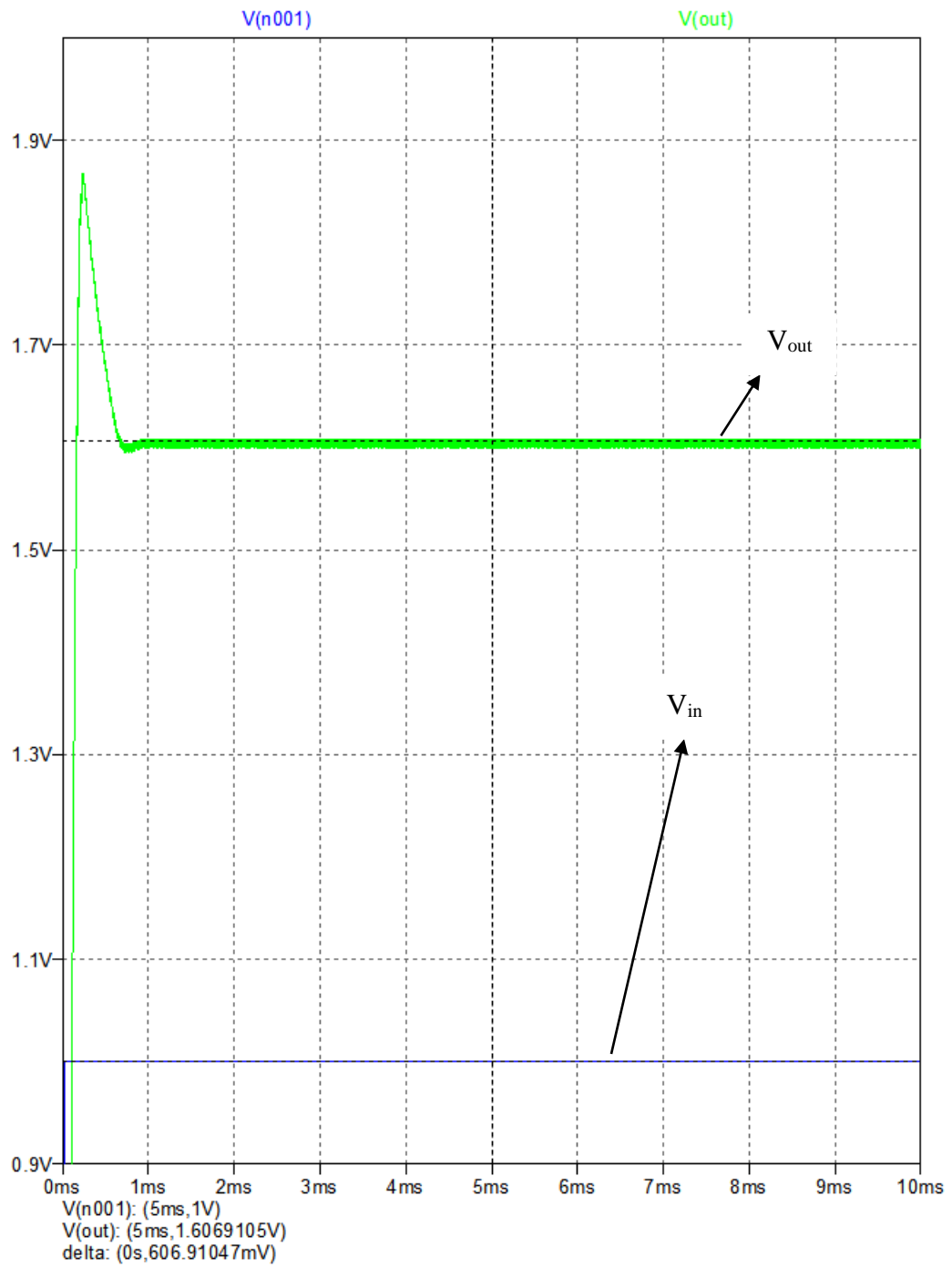


Figure 21: Graph of V_{out} and V_{in} for simulated boost converter circuit

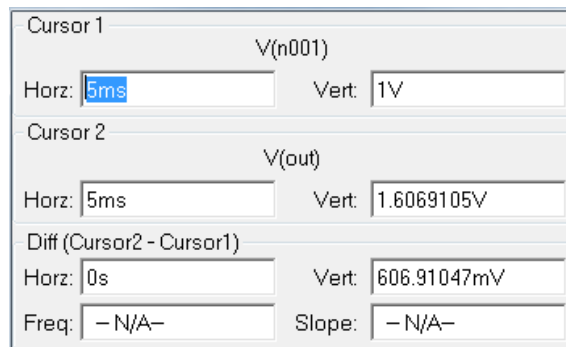


Figure 22: Voltage values for both V_{in} (V(n001)) and V_{out} (V(out)) for boost converter

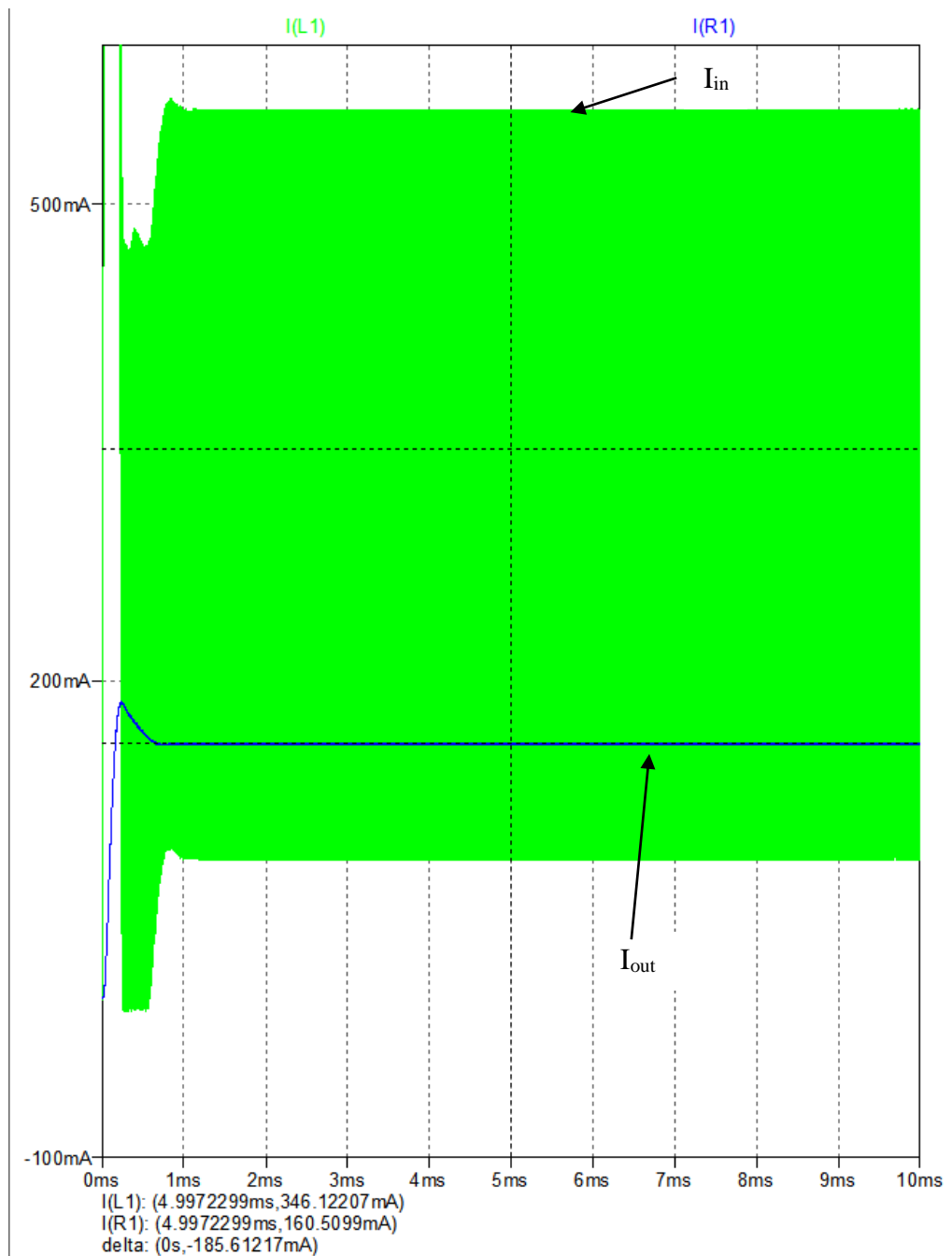


Figure 23: Graph of I_{out} [I(R1)] and I_{in} [I(L1)] for simulated boost converter circuit

In Figure 21, $V(n001)$ is the V_{in} while $V(out)$ is the V_{out} for the circuit. Similarly, a buck converter is also simulated using LTSpice and the schematic diagram is as shown in Figure 24.

Buck Converter

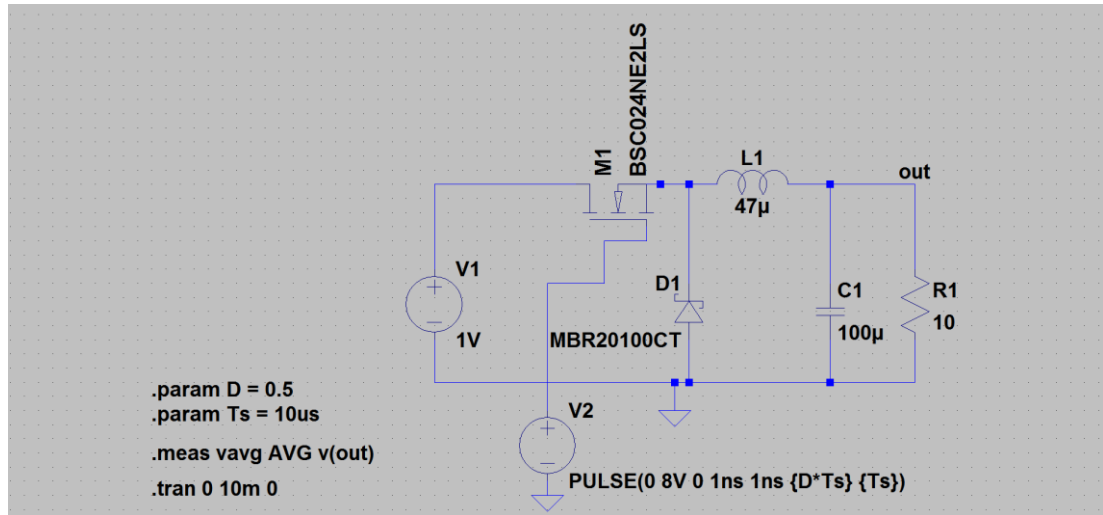


Figure 24: Schematic diagram for simulated buck converter using LTSpice

Similarly, the simulation was run to obtain voltage readings as shown in Figure 25 and the graph of V_{out} and V_{in} for the simulated circuit was obtained as shown in Figure 26.

Cursor 1	
V(out)	
Horz: 4.8ms	Vert: 347.2003mV
Cursor 2	
V(n001)	
Horz: 4.8ms	Vert: 1V
Diff (Cursor2 - Cursor1)	
Horz: 0s	Vert: 652.7997mV
Freq: - N/A -	Slope: - N/A -

Figure 25: Voltage values for both V_{in} ($V(n001)$) and V_{out} ($V(out)$) for buck converter

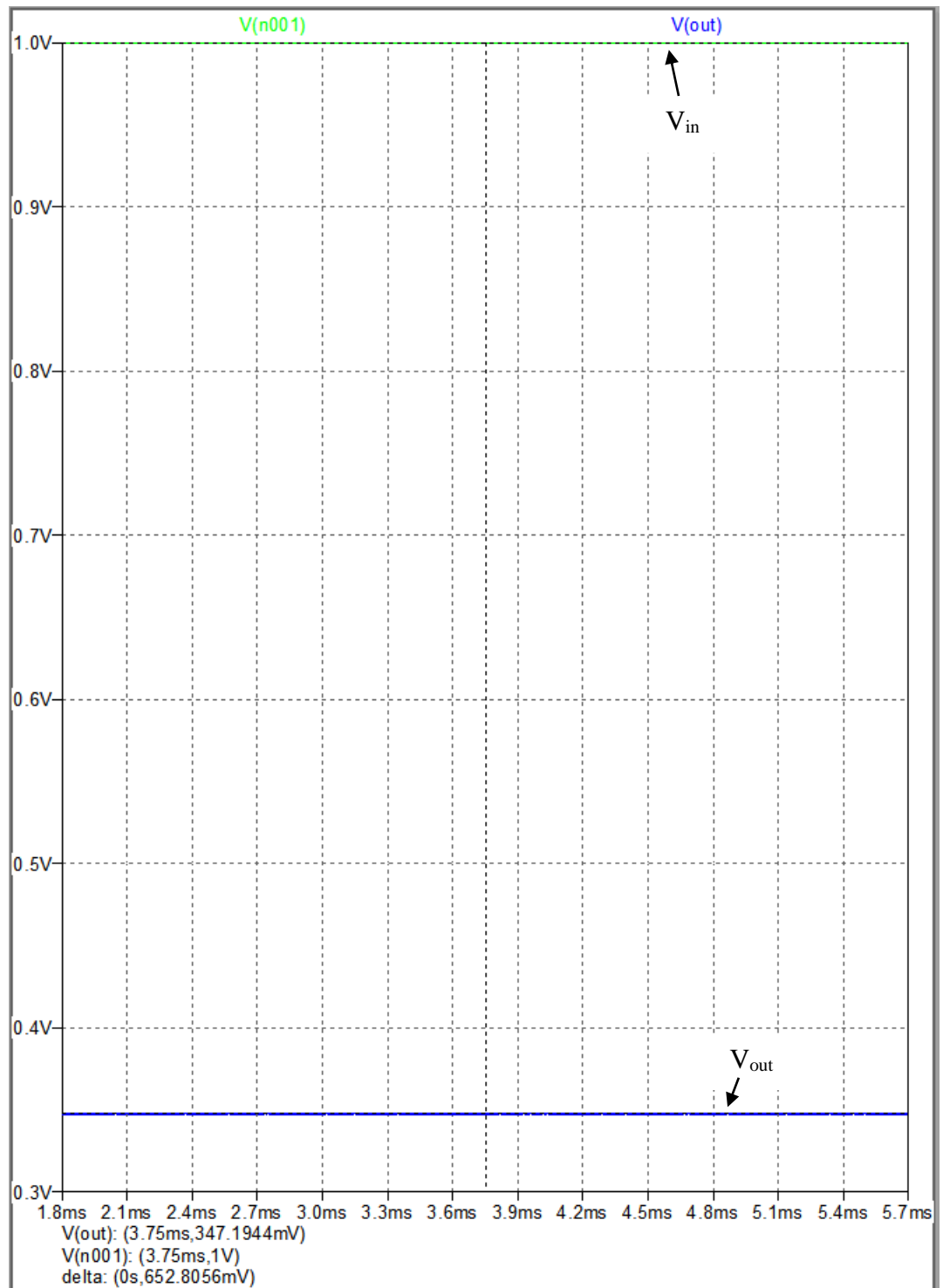


Figure 26: Graph of V_{in} and V_{out} for simulated buck converter circuit

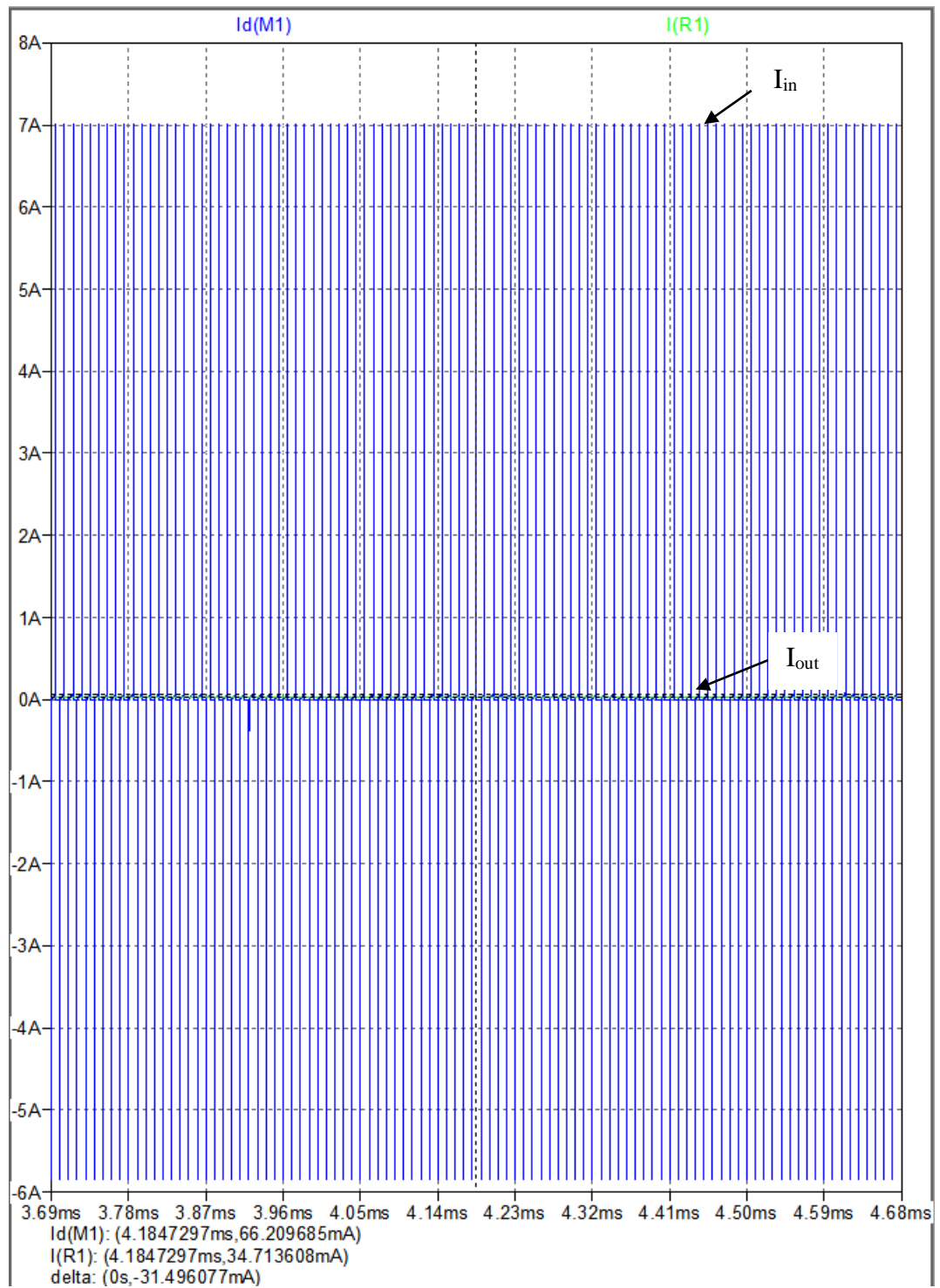


Figure 27: Graph of I_{out} [$I(R1)$] and I_{in} [$I_d(M1)$] for simulated buck converter circuit

4.3 Circuit Implementation Results

The simulated circuit in 4.2 were physically implemented using components as listed in Methodology section. The boost circuit was implemented on a Veroboard in order to obtain experimental results for comparison between experimental value and simulated value from LTSpice. Figure 28 shows the implemented boost converter.

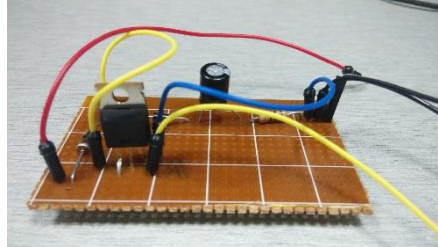


Figure 28: Implemented boost converter

The input voltage to the boost converter was 1.025V, obtained from the voltage supply as shown in the Figure 29. The output voltage, 1.258V was measured using multimeter as shown in Figure 30.

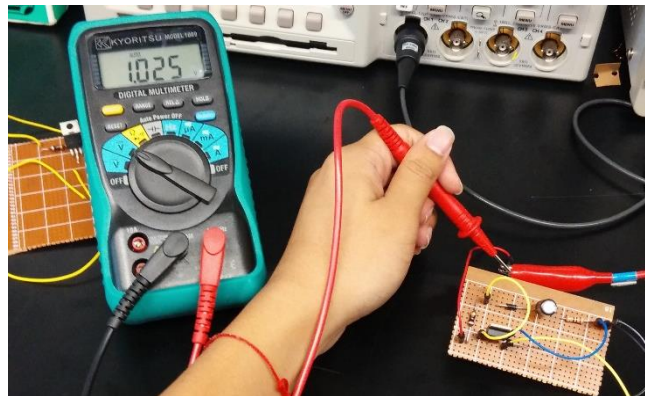


Figure 29: Input voltage of 1.025V measured

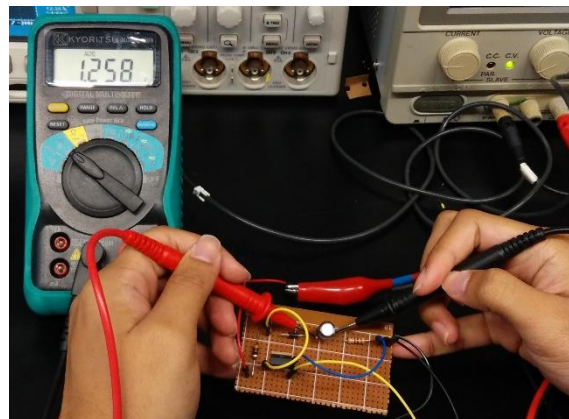


Figure 30: Output voltage of 1.258V measured

Several readings were taken for the input and output voltage of the boost converter. The input voltages and output voltages were recorded and tabulated into Table 6.

Table 6: Voltage, current, power and efficiency for designed boost converter

Readings	Input Voltage (V)	Input Current (mA)	Input Power (mW)	Output Voltage (V)	Output Current (mA)	Output Power (mW)	Efficiency (%)
1	1.025	0.265	0.272	1.258	0.138	0.174	38.17
2	1.022	0.254	0.260	1.256	0.128	0.161	
3	1.019	0.248	0.253	1.251	0.121	0.151	
Average	1.022	0.257	0.262	1.255	0.129	0.162	

4.4 Discussion

For the experimental results, several graphs were plotted based on the voltage and current readings obtained. There were three graphs with different variables tested in each graph. For the graph of voltage against time for different concentration of solute as shown in Figure 31, a trend was observed in which the higher the concentration, the higher the output voltage obtained. However, the difference in output voltage is minimal. Another trend observed was that the output voltage depreciated at a higher rate in the solution with lower concentration of solute. This means that the cell works longer in saturated electrolyte as compared to low saturation of electrolyte. In low saturation electrolyte, the output voltage dropped at an alarming rate with each passing time. After 30 minutes, the voltage drop was more than half the original output voltage obtained. It can be concluded that the optimum concentration of the cell is around 1.677 M in which the salt water electrolyte reaches saturation.

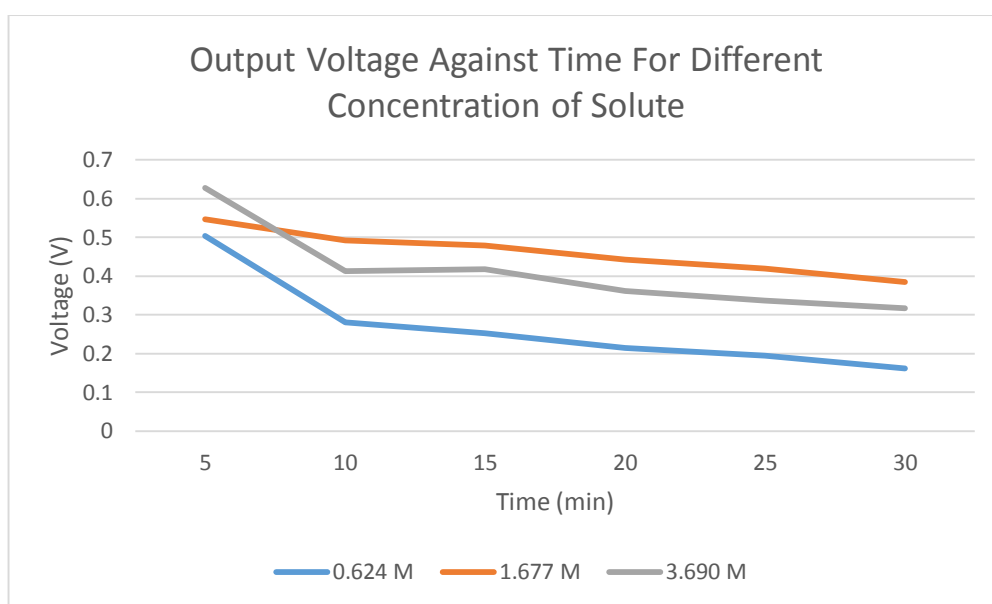


Figure 31: Graph of output voltage against time for different concentration of solute

The second graph plotted was the graph of voltage against time for different volume of water. In this graph shown in Figure 32, the volume of water was varied and the output voltage of the cell was observed. From the graph, it is shown that the volume of water for the electrolyte did not affect the amplitude of the output voltage as time increases.

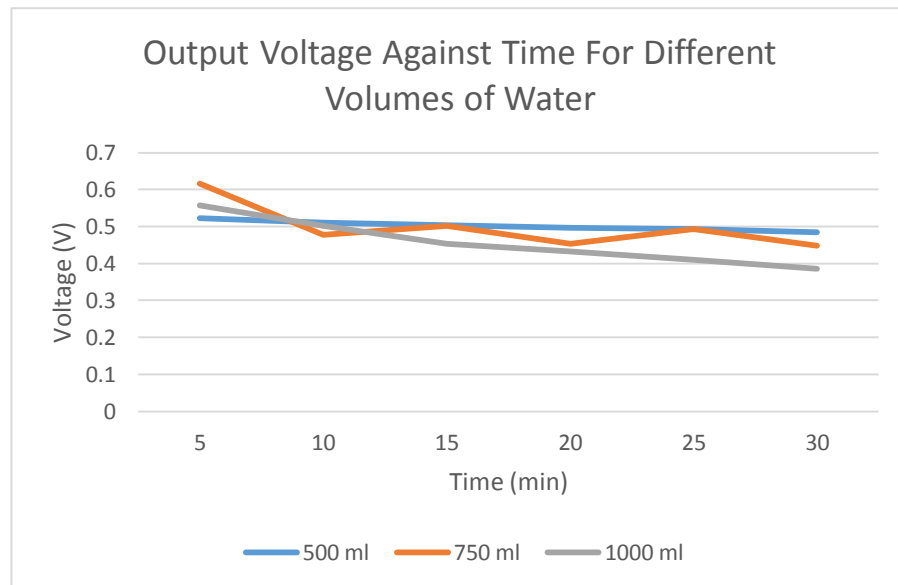


Figure 32: Graph of output voltage against time for different volumes of water

Figure 33 depicted the output voltage against time for different types of electrolytes. NaCl solution were compared with other types of electrolyte such as water and combination of water and acetic acid. The electrolyte of water and vinegar provided the highest output voltage, reaching almost 0.8V. Even though the water electrolyte shows higher output voltage than the NaCl solution, it can be observed that the output current was 0A for the water electrolyte. This is due low conductivity of water preventing current from flowing. Hence, water and vinegar is the best electrolyte.

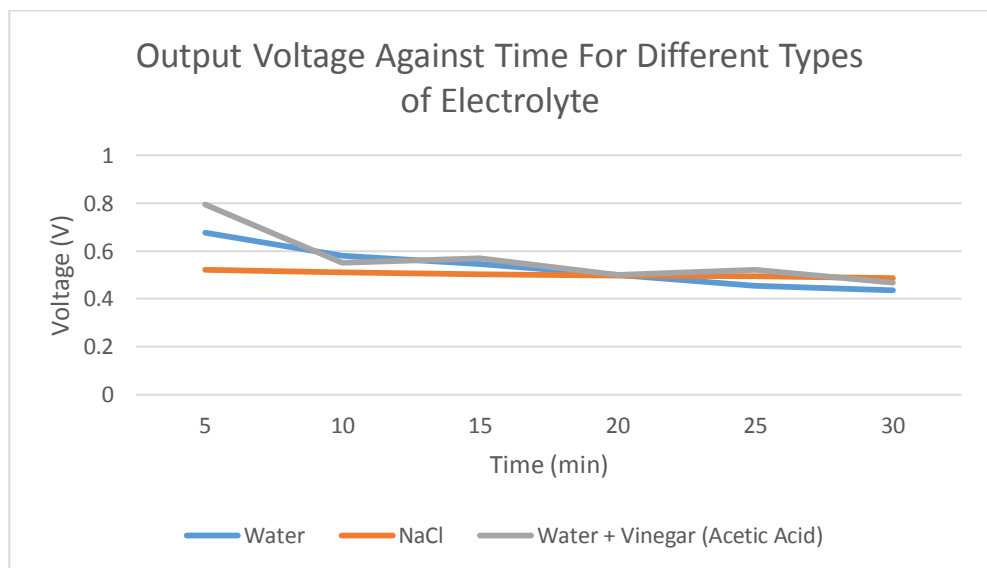


Figure 33: Graph of output voltage against time for different types of electrolyte

Three graphs of output power against time was also plotted for the three different variables. In Figure 34, it can be observed that higher concentration of solute provides higher output power. However, this is true only for the initial 5 minutes of operation. After 5 minutes, the output power for both 1.677 M and 3.69 M was similar. This means that the optimal concentration of solute for the cell would be 1.677 M.

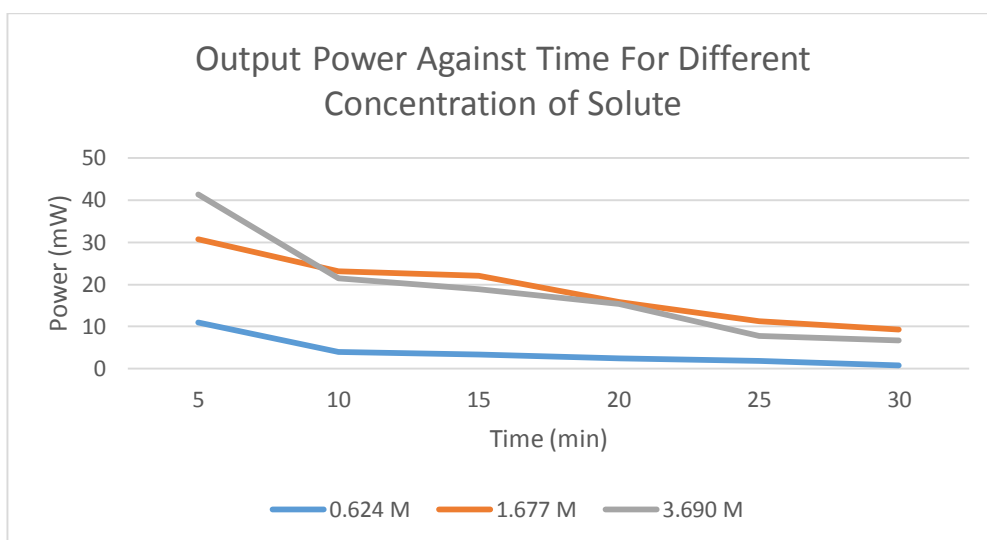


Figure 34: Graph of output power against time for different concentration of solute

For Figure 35, the volume of the water did not affect much on the output power. The deviation in output power between these different volumes of water was due to human error during measurement done on the experimental setup.

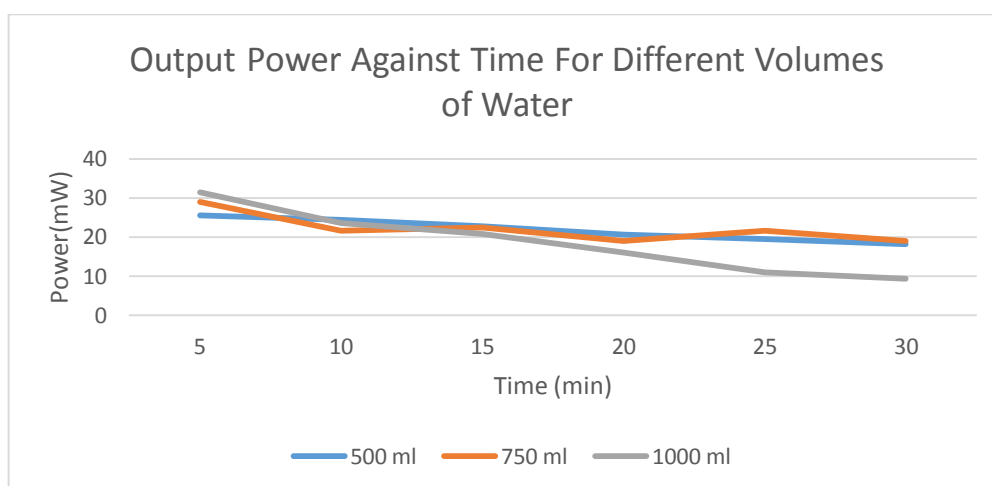


Figure 35: Graph of output power against time for different volume of water

Figure 36 represents the graph of output power against time for three different solutes, which were water, salt solution and water mixed with vinegar. The highest output power achievable was the mixture of water and vinegar. The salt solution provided the most stable output power among all three electrolytes. Water did not provide any output power due to the inability of water as an electrolyte.

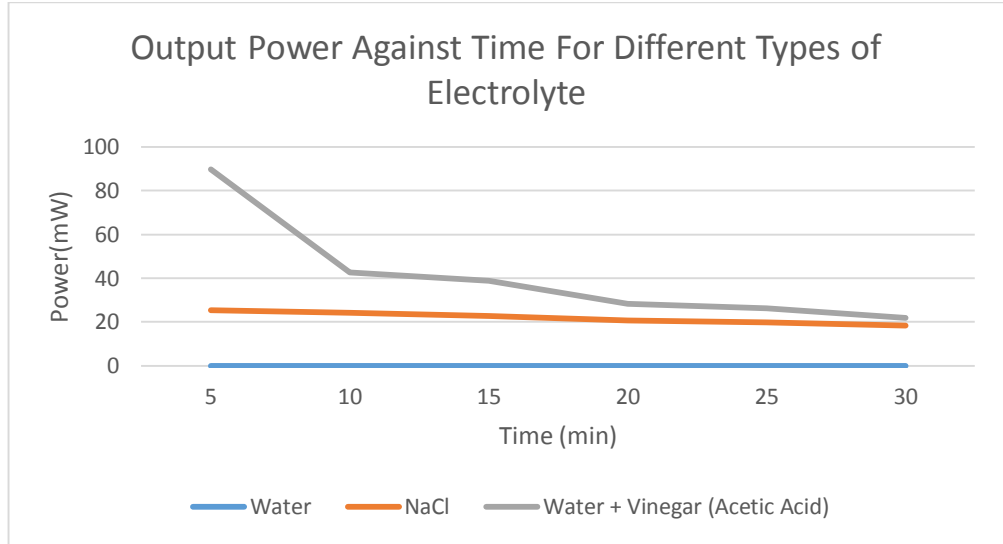


Figure 36: Graph of output power against time for different types of electrolyte

The average output voltage obtained is around 0.5 – 0.7V for each cell. Since the voltage obtained per cell is only ~0.5V, we need to boost the voltage to a higher voltage. By combining two of these cells, up to 1V can be achieved. This 1V can be boosted to 3.3V or 5V using a DC-DC boost converter circuit for powering sensor nodes that requires higher voltage but lower current. So, a boost converter will be chosen instead of a buck converter due to the already low voltage produced by the cell.

In the circuit simulation results, the boost converter is able to boost the 1V supplied to 1.61V. The theoretical voltage calculated is 2V with duty ratio, $D = 0.5$ in accordance to the equation:

$$\frac{V_o}{V_s} = \frac{1}{1-D} = \frac{1}{1-0.5} = 2$$

$$V_o = V_s \left(\frac{1}{1-D} \right) = (1V)(2) = 2V$$

The output voltage obtained was not exactly 2V due to switching losses and other external factors.

For the buck converter, an input voltage of 1V was also used and an output voltage of 0.347V was obtained. The ideal output voltage obtained would be 0.5V according to the following equation:

$$\frac{V_o}{V_s} = D = 0.5$$

$$V_o = V_s D = (1V)(0.5) = 0.5V$$

Due to switching losses, the output voltage dropped to 0.347V from 0.5V.

For the physical implementation of the boost converter circuit, an average of 1.255V output voltage was obtained from an input voltage of 1.022. Based on the equation above, with a duty ratio of 50%, the theoretical output voltage obtained should be 2.044V. This means that the boost converter tested has an efficiency of 38.6% for stepping up voltage based on the following equation:

$$\begin{aligned} \text{Step up efficiency} &= \frac{\text{Theoretical } V_{out} - \text{Experimental } V_{out}}{\text{Theoretical } V_{out}} \times 100\% \\ &= \frac{2.044 - 1.255}{2.044} \times 100\% = 38.6\% \end{aligned}$$

In terms of efficiency for power, the output power obtained was 0.162W from an input power of 0.262W. This means that 0.1W was lost due to switching losses and other factors. The efficiency for power was calculated with following equation:

$$\begin{aligned} \text{Overall efficiency (Power)} &= \frac{\text{Input power, } P_{in} - \text{Output power, } P_{out}}{\text{Input power, } P_{in}} \times 100\% \\ &= \frac{0.262 - 0.162}{0.262} \times 100\% = 38.17\% \end{aligned}$$

The output power per square centimeter was calculated to be:

$$\text{Output power per square centimeter} = \frac{89.7mW}{135 \text{ cm}^2} = 0.664 \text{ mW/cm}^2$$

CHAPTER 5

CONCLUSION AND RECOMMENDATIONS

Based on the comparison of techniques in literature review of this research paper, mixing entropy battery was chosen as the technique for the experimental part of this research paper. Using dissimilar materials with different electrical potential for the anode and cathode electrodes such as aluminium and carbon, an experiment was conducted. Different variables such as volume of water, concentration of solute and type of electrolyte were tested in order to study their effects on the efficiency of the cell. It was found that volume of water does not affect the cell but the concentration of the solute is crucial for the cell. Besides that, the mixture of water and vinegar (acetic acid) was found to be the best electrolyte among all three different electrolytes used. The highest achievable output power was 89.7mW which is high enough to power low-power sensors.

A DC-DC boost converter will also be used to step-up the voltage. The converter will be designed thorough simulation using LTSpice. Based on the simulation done, the boost converter was able to boost supply voltage of 1V to 1.61V. Physical implementation of the circuit was done and the circuit was tested in which an input voltage of 1.022V was boosted to 1.255V. The efficiency of the boost converter was 38.17% based on input power and output power obtained. The output power per square centimeter was also calculated to be 0.664mW / cm², which is economically viable.

The output voltage and output current can be further increased or optimized. By using different configurations of placement for the electrodes, the surface area of the carbon can be increased which will increase the current obtained. Besides that, several cells can also be produced and connected in series to obtain higher voltage from the setup for higher voltage uses.

References

- [1] J. W. Post, J. Veerman, H. V. M. Hamelers, G. J. W. Euverink, S. J. Metz, K. Nijmeijer, *et al.*, "Salinity-gradient power: Evaluation of pressure-retarded osmosis and reverse electrodialysis," *Journal of Membrane Science*, vol. 288, pp. 218-230, 2/1/ 2007.
- [2] A. T. Jones and W. Finley, "Recent development in salinity gradient power," in *OCEANS 2003. Proceedings*, 2003, pp. 2284-2287 Vol.4.
- [3] G. L. Wick and W. R. Schmitt, "PROSPECTS FOR RENEWABLE ENERGY FROM THE SEA," *Marine Technology Society Journal*, vol. 11, pp. 16-21, 1977.
- [4] D. A. Vermaas, E. Guler, M. Saakes, and K. Nijmeijer, "Theoretical power density from salinity gradients using reverse electrodialysis," *Energy Procedia*, vol. 20, pp. 170-184, 2012.
- [5] Z. Jia, B. Wang, S. Song, and Y. Fan, "Blue energy: Current technologies for sustainable power generation from water salinity gradient," *Renewable and Sustainable Energy Reviews*, vol. 31, pp. 91-100, 3// 2014.
- [6] M. F. M. Bijmans, O. S. Burheim, M. Bryjak, A. Delgado, P. Hack, F. Mantegazza, *et al.*, "CAPMIX -Deploying Capacitors for Salt Gradient Power Extraction," *Energy Procedia*, vol. 20, pp. 108-115, 2012.
- [7] B. B. Sales, F. Liu, O. Schaetzle, C. J. N. Buisman, and H. V. M. Hamelers, "Electrochemical characterization of a supercapacitor flow cell for power production from salinity gradients," *Electrochimica Acta*, vol. 86, pp. 298-304, 12/30/ 2012.
- [8] K. Gerstandt, K. V. Peinemann, S. E. Skilhagen, T. Thorsen, and T. Holt, "Membrane processes in energy supply for an osmotic power plant," *Desalination*, vol. 224, pp. 64-70, 4/15/ 2008.
- [9] T. Thorsen and T. Holt, "The potential for power production from salinity gradients by pressure retarded osmosis," *Journal of Membrane Science*, vol. 335, pp. 103-110, 6/15/ 2009.
- [10] M. Kurihara and M. Hanakawa, "Mega-ton Water System: Japanese national research and development project on seawater desalination and wastewater reclamation," *Desalination*, vol. 308, pp. 131-137, 1/2/ 2013.
- [11] R. E. Pattle, "Production of Electric Power by mixing Fresh and Salt Water in the Hydroelectric Pile," *Nature*, vol. 174, pp. 660-660, 10/02/print 1954.
- [12] C. J. N. B. Olivier Schaetzle, "Salinity Gradient Energy: Current State and New Trends," *Engineering*, vol. 1, pp. 164-166, 2015-06-04 2015.
- [13] D. Brogioli, R. Ziano, R. A. Rica, D. Salerno, and F. Mantegazza, "Capacitive mixing for the extraction of energy from salinity differences: Survey of experimental results and electrochemical models," *Journal of Colloid and Interface Science*, vol. 407, pp. 457-466, 10/1/ 2013.
- [14] D. Brogioli, R. Ziano, R. A. Rica, D. Salerno, O. Kozynchenko, H. V. M. Hamelers, *et al.*, "Exploiting the spontaneous potential of the electrodes used in the capacitive mixing technique for the extraction of energy from salinity difference," *Energy & Environmental Science*, vol. 5, pp. 9870-9880, 2012.
- [15] B. B. Sales, M. Saakes, J. W. Post, C. J. N. Buisman, P. M. Biesheuvel, and H. V. M. Hamelers, "Direct Power Production from a Water Salinity Difference in a Membrane-Modified Supercapacitor Flow Cell," *Environmental Science & Technology*, vol. 44, pp. 5661-5665, 2010/07/15 2010.
- [16] M. Marino, L. Misuri, M. L. Jiménez, S. Ahualli, O. Kozynchenko, S. Tennison, *et al.*, "Modification of the surface of activated carbon electrodes for capacitive mixing energy extraction from salinity differences," *Journal of Colloid and Interface Science*, vol. 436, pp. 146-153, 12/15/ 2014.

- [17] F. La Mantia, M. Pasta, H. D. Deshazer, B. E. Logan, and Y. Cui, "Batteries for Efficient Energy Extraction from a Water Salinity Difference," *Nano Letters*, vol. 11, pp. 1810-1813, 2011/04/13 2011.
- [18] N. A. C. Mustapha, A. H. M. Z. Alam, S. Khan, and A. W. Azman, "Boost converter for low voltage energy harvesting applications: Basic component selection," in *Smart Instrumentation, Measurement and Applications (ICSIMA), 2013 IEEE International Conference on*, 2013, pp. 1-4.
- [19] M. H. Rashid, *Power Electronics Handbook*: Academic Press, 2001.
- [20] M. R. Sarker, S. H. M. Ali, M. Othman, and M. S. Islam, "Designing a low voltage energy harvesting circuits for rectified storage voltage using vibrating piezoelectric," in *Research and Development (SCOReD), 2011 IEEE Student Conference on*, 2011, pp. 343-346.
- [21] D. Dondi, A. Bertacchini, L. Larcher, P. Pavan, D. Brunelli, and L. Benini, "A solar energy harvesting circuit for low power applications," in *2008 IEEE International Conference on Sustainable Energy Technologies*, 2008, pp. 945-949.